Electric Power Systems Research 117 (2014) 36–46

Contents lists available at ScienceDirect

Electric Power Systems Research

journal homepage: www.elsevier.com/locate/epsr

Unlocking distribution network capacity through real-time thermal rating for high penetration of DGs

M.Z. Degefa *, M. Humayun, A. Safdarian, M. Koivisto, R.J. Millar, M. Lehtonen

Department of Electrical Engineering and Automation, Aalto University, Espoo, Finland

ARTICLE INFO

Article history:
Received 5 December 2013
Received in revised form 12 May 2014
Accepted 31 July 2014
Available online 28 August 2014

Keywords:
Active network management
Distributed generation control
Load forecasting
Power flow
Real-time thermal rating
State estimation

ABSTRACT

Highly stochastic loading in the emerging active distribution networks means that electric utilities need to use their assets to the fullest by deploying intelligent network management tools. Real-time thermal rating (RTTR) provides possibility for short term and even real-time active distribution network management enabling the network to run closer to an overload state without damage. In this study, a RTTR based active distribution network management framework is formulated giving hour-by-hour network capacity limits. Relationships of stochasticities in customer loads and DG output with thermal responses of underground cables, overhead lines and distribution transformers are explained. RTTR is applied on all distribution network components with simulated scenarios involving various levels of DG penetration. This study quantifies the potential for an increased DG utilization and an increased potential for new DG installations when RTTR is integrated with distribution management systems.

1. Introduction

An increasing number of renewable energy resources are being installed in distribution systems. Larger units, usually above 10 MW, are installed by commercial power producers and are generally connected to transmission facilities. Smaller units which are no larger than 1 or 2 MW are, however, installed in distribution systems and referred to as 'distributed generation' (DG) [1]. It is anticipated that with the proliferation of DG some distribution networks will face power flow congestion due to the thermally vulnerable components restricting the connection capacity and active energy yield of DG [2]. In addition, switching operations that reconfigure the feeder will be common in distribution systems with the advent of DGs [3].

Nevertheless, traditionally, the main task of distribution system analysis tools has been to solve the power flow for one specific point in time, which is the predicted peak demand. To increase DG connectivity and also to harness the generated renewable energy efficiently there is a need for active distribution management systems (DMS). It is also in the interest of distribution network operators (DNOs) to increase asset utilization in a safe manner, potentially allowing latent capacity to be used under strictly controlled conditions [2]. Currently, the thermal limits applied by DNOs tend to be based on fixed or assumed meteorological conditions that are not always accurate representations of the actual operating conditions [4], the result of which is potentially a conservative constraint on power flows. In place of the rigid capacity planning rules, the planning process needs to incorporate more detailed simulations of capacity constraints. Hence a modeling analysis including dynamic thermal models is expected to be a strong component in an active distribution network management system.

In this regard, the application of continuously changing (rather than seasonal) ratings, which can be updated in real-time, could enable generators to enhance their energy export, defer network reinforcement and also allow increased access to distribution networks for weather dependent forms of generation. Integrating real-time thermal rating in active power flow management schemes has been a research topic among the power systems research community for a long time. EPRI's dynamic thermal circuit rating system released in early 1999 was among the first attempts which tried to realize the higher equipment utilization offered by dynamic thermal rating [5]. Another methodology to forecast the real-time thermal rating of overhead lines, presented in [6], promises enhanced network operator decision making capabilities regarding network power flow management.

In [7], in addition to investment options such as substation or feeder expansions, installations of new DGs are presented as alternatives for utilities to solve network capacity limits. Nevertheless, it is also mentioned in [7] that on shorter feeders the ampacity limits could prohibit the utilization of economically beneficial DG installations. In [8], it is demonstrated that without careful engineering assessments, increased DG installations may have adverse

* Corresponding author. Tel.: +358 44 5654598; fax: +358 9 470 2991.
E-mail address: merkebu.degefa@aalto.fi (M.Z. Degefa).

http://dx.doi.org/10.1016/j.epsr.2014.07.032

system effects, such as exposing system and customer equipment to potential damages. The optimization of power output from DGs within a distribution network while maintaining thermal limits is proposed in [9]. In [10], a day-ahead scheduler which considers capacity limits in the form of a specific upper bound to the current amplitude is proposed. The scheduling procedure in [10] solves a non-linear multi-objective problem for the optimization of distributed resource production during the following day. A thermal state estimation based DG output control algorithm for a wide area network power flow control is proposed in [11]. The study in [11] verifies the real-time rating system is able to estimate conductor temperature with an average error in the range of −2.2 °C to +1.4 °C.

Despite the numerous studies, the relationship between thermal states and stochastic DG generation has not been studied or quantified clearly. Due to the variations of thermal time constants among overhead lines, underground cables and transformers the thermal responses also differ accordingly. Hence a look into the entire distribution network is necessary to identify potential bottlenecks with increased installations of DG. An hour ahead thermal capacity limit forecasting used for optimal scheduling of DGs entirely based on thermal, DG and load models is presented in this paper. The contribution of this paper is the quantification of the benefits of real-time thermal rating for the efficient utilization and increased integration of DGs. The RTTR technique is simulated on atypical Finnish MV test network covering an approximately 7.5 km^2 residential area.

There are two specific issues addressed in this study. First the unused DG potential, for example, the fact that the generation of some renewable energy plants that produce but cannot store energy is requested to be curtailed when grid limits are violated. The second is the demand for expensive upgrading of the distribution network for the integration of new DGs. Solving the mentioned problems requires the merging of planning and real-time analysis which is listed as a key challenge for future distribution system analysis tools in [3]. These concerns are addressed through the proposal and implementation of a non-conservative real-time thermal rating system with hourly update of the electro-thermal behavior of the network. Within the scope of this study, the RTTR technique involves real-time measurement of component temperatures and external parameters, such as air temperature or wind speed, in order to estimate component real-time thermal state and rating.

The proposed RTTR procedure can be used as a strong component in active distribution management systems. It also naturally integrates with DG control architecture and optimal power flow (OPF) functions. The optimal power flow in this study takes the input of hourly updated capacities of overhead lines, underground cables and transformers, while minimizing the total cost of load curtailment (could also be demand response action) and DG curtailment. The proposed procedure performs hour ahead forecasts of load demand, DG output and the subsequent real-time thermal rating of the distribution network based on hour-ahead weather forecasting. Through a cost function, the impact of RTTR is compared with static rating for increased network capacity, better integration and efficient utilization of DGs over a one year time window.

Considering the model based analysis framework presented in this study, brief explanations on thermal models, load models and DG models are presented in order to show how they have been utilized in this study. Section 2 presents the test distribution network for a typical Finnish suburban residential area used in this study. Dynamic thermal rating essentials are presented in Section 3, where component thermal modeling procedures are described. Besides, in this section, the usual rating scenario in today's distribution network is explained. In Section 4, load and generation forecasting methods are discussed and Section 5 presents the framework for the real-time thermal rating of a distribution network. After discussing and comparing static rating to real-time thermal rating in Section 6, Section 7 summarizes the key findings and points out the relevant issues for future studies.

Table 1
Radial distribution network data.

1 Primary substation (40 MVA, 110/20 kV)	
16 secondary substations (1.6 MVA, 20/0.4 kV)	
Heating type	No.
1800 households	
Direct electric (DE)	673
District heating (DIST)	960
Ground source HP (GSHP)	109
Electric storage heating (STORE)	58

2. Test distribution network

The test network was planned for residential buildings with a network planning algorithm in the Aalto University power systems laboratory using data from the Kainuu area in central Finland [12]. It is supplying about 1800 households belonging to four heating system groups, as shown in Table 1. In the test network all nodes except for the primary substation are secondary substations supplying LV connected households. Substations (transformers) are labeled with numbers and line sections are referenced by the node they are supplying. Line sections 14 and 2 are overhead bare conductor lines but all other line sections are underground MV cables installed inside unfilled conduit, which itself is buried 0.7 m below the surface. Solar panels are connected to the LV network behind transformers 10 and 12. Wind turbines are connected to the MV network at secondary substations 12 and 14, with proportions of 2% and 98%, respectively, of the total wind turbine connections in the distribution network. There are reserve connections between secondary substations 12 and 9 as well as between 6 and 3, normally operating in open mode. As can be seen in Fig. 1, the test network operates radially. The suburban network in Fig. 1 has short lines and therefore the voltage drop is small and is not a limiting factor in this study.

The four heating type households have very distinct load behavior, as shown in Fig. 2. All electric power consuming heating types have higher consumption and changes within a year following a similar trend to ambient temperature. Besides, due to the charging and discharging behavior of electric storage heaters, daily peak loadings are visible at certain hours of the day, whereas ground source heat pumps have a spike in consumption whenever the supportive direct electric heating switches on. These distinct behavioral patterns have a cumulative effect on substation loading based on their magnitude, as shown in Table 2.

The one year hourly data used in this study is for central Finland and it includes AMR metered household load, ambient temperature, solar irradiation and wind speed. A database of actual household AMR metered hourly energy consumption data is used to randomly populate the load of the four household types in a certain geographical area. The network planning algorithm connected these households, under 16 secondary substations, with the proportions shown in Table 2. The straight line network diagram for the MV network side is presented in Fig. 1, with the underlying LV network shown faintly.

3. Dynamic thermal ratings

Static distribution system ratings are usually calculated assuming conservative weather conditions, for instance, for overhead lines, low wind speed conditions and high ambient temperature. The ratings are usually provided for the different seasons in a year. Besides ratings supplied by the over-head line manufacturer,

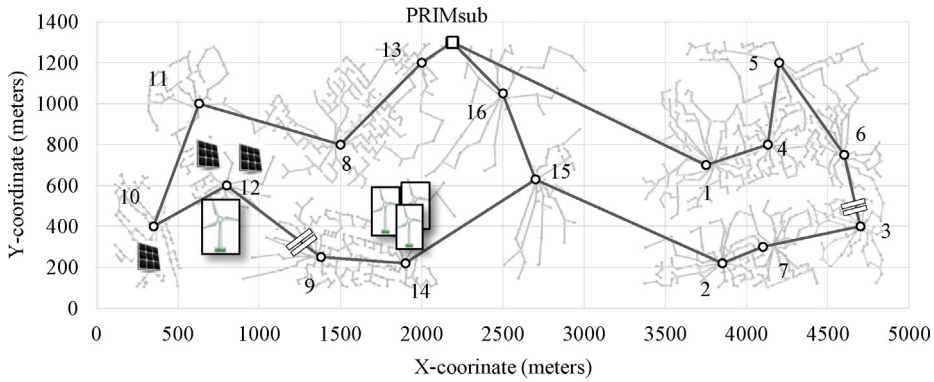

Fig. 1. MV distribution network plan supplying 1800 households.

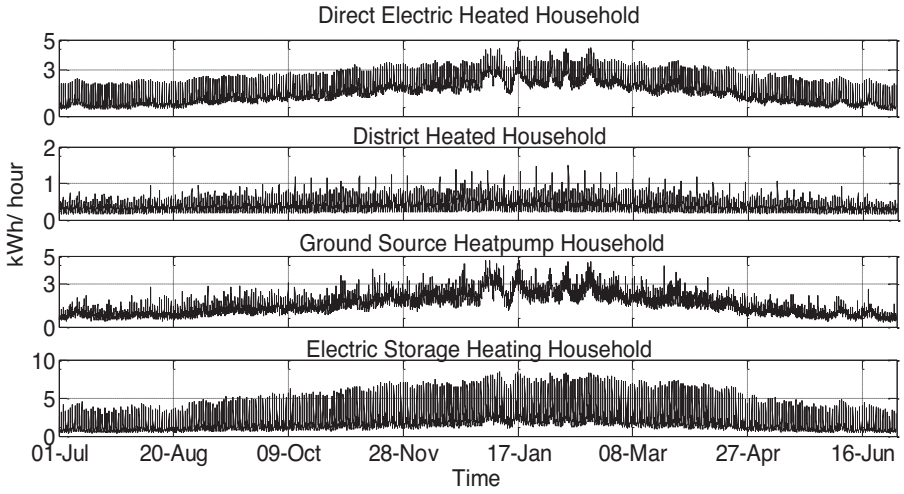

Fig. 2. Household types and their typical hourly load profile for one year (July, 2008 to June, 2009).

distribution system operators use their own experience in either increasing or decreasing ratings depending on the operating environmental conditions. The loading guides of international standard organizations, such as IEC and IEEE, are the main guides for system operators. IEEE Std C57.91-2011, for instance, is one such organization detailing loading guidelines for oil-immersed transformers [13]. According to [13], a continuous hottest-spot temperature of 110 °C can be handled with normal life expectancy. Emergency loadings up to 200 °C hottest-spot temperature can be applied; however this would incur 1% loss of life per emergency if the emergency loading is maintained for 1 h. Hence, in this study dynamic thermal rating utilization is considered in real-time normal network operation where the compromise of loss of life is avoided.

Table 2
Distribution of LV customers into the four heating types under the sixteen secondary substations.

No.	DE	DIST	GSHP	STORE
1	151	6	0	0
2	116	0	0	0
3	85	0	0	0
4	101	0	0	0
5	20	75	0	0
6	101	8	0	0
7	99	0	0	0
8	0	213	0	5
9	0	126	0	26
10	0	150	0	0
11	0	84	0	0
12	0	70	0	27
13	0	105	3	0
14	0	119	4	0
15	0	0	56	0
16	0	4	46	0

Component thermal models are pre-requested for a power system real-time thermal rating. In this study the three major distribution network components are used to compute the system rating. These components are overhead lines, electric cables and power transformers, and their respective thermal models are used. Except for cables buried inside unfilled conduit and secondary transformers installed in cabins, IEEE standards are used to develop the thermal models. For cables inside unfilled conduit a suitable air-gap thermal model has been proposed by the authors in [14]. A dynamic thermal model for prefabricated MV/LV substations, presented in [15], is used for secondary substation transformer thermal ratings.

3.1. Component thermal modeling

The component models can either be dynamic or static. The dynamic model involves time constants, which are functions of thermal resistances and capacitances emulating the transient responses. The time constant for overhead bare lines is very small, as the maximum possible hotspot steady state temperature for a given loading scenario shows up in the order of minutes. IEEE standard [16] is used for the thermal modeling of overhead lines and [13] is used for oil-immersed distribution transformer indoor installations. However, for underground cables installed inside

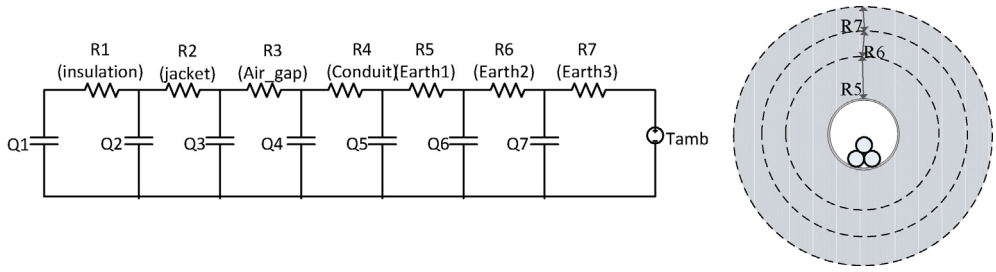

Fig. 3. Seven loop thermal model for underground cable inside unfilled conduit.

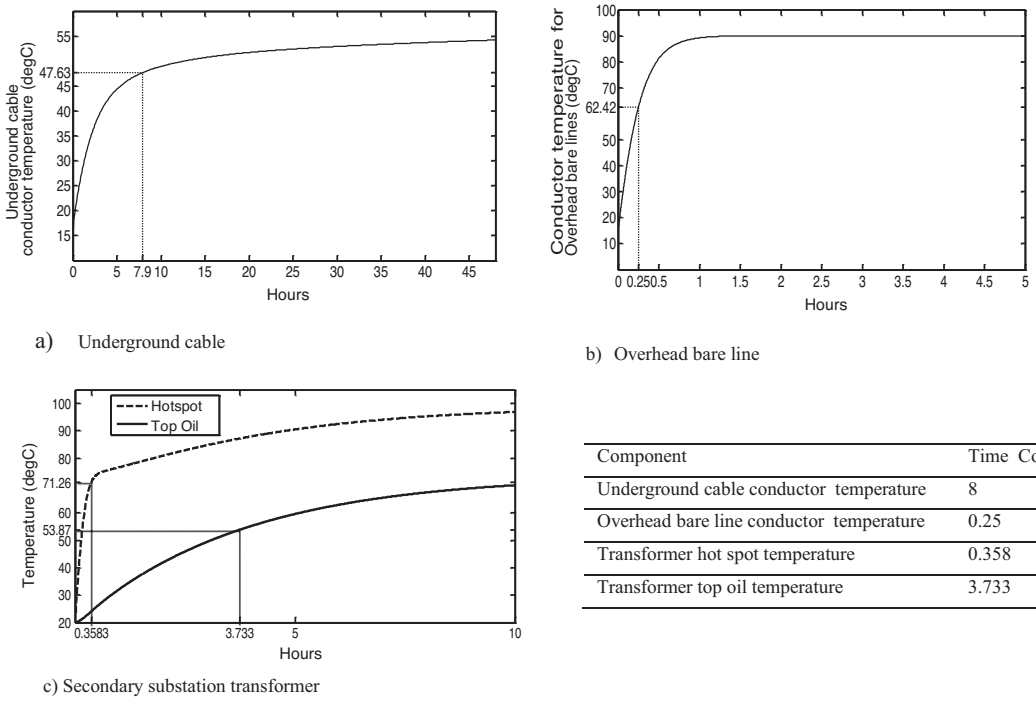

Component	Time Constant (hours)
Underground cable conductor temperature	8
Overhead bare line conductor temperature	0.25
Transformer hot spot temperature	0.358
Transformer top oil temperature	3.733

Fig. 4. Time constants of the typical distribution network components used in this study for rated step loading from cold start.

buried air filled conduit, a seven loop dynamic thermal model is used, which has been developed by the authors in Aalto University [14,17]. For better visualization of the dynamism, the thermal-electric analogy circuits of the components are presented in Fig. 3.

By definition, a thermal time constant is the amount of time necessary for a particular body or system to change to 63.2% of the total difference between its initial and final body temperatures when it is subjected to a step change in load. The three components in a distribution system network have very different time constants, which can be translated as how fast the component responds to favorable or unfavorable environmental conditions. Components with high time constants reach the hotspot temperature increment corresponding to temporary overloading in the very far future. Besides, the future response of such components is strongly influenced by their past thermal-loading history. The advantage of a high time constant is the ability to handle high over loading followed by an extended period of normal loading. Contrary to that, low time constants have the advantage of fast response to favorable (cooling) environmental conditions, such as high wind speed for overhead bare lines. For transformers, the hotspot temperature time constant is usually a few minutes whereas for top oil temperature the time constant is in hours. The time constants for underground cables are the highest, giving the potential for temporary overloading, whereas for overhead lines the time constant is the lowest, giving most opportunity when overloading and favorable environmental conditions are coinciding (see Fig. 4). All the thermal models are based on real-time ambient temperature and therefore measurements for the ambient temperature are assumed to be readily available.

Based on hourly Finnish weather data, Fig. 5 shows the hourly rating of an overhead line with the parameters shown in Appendix A. It is compared with seasonal static ratings. Fig. 6 shows the

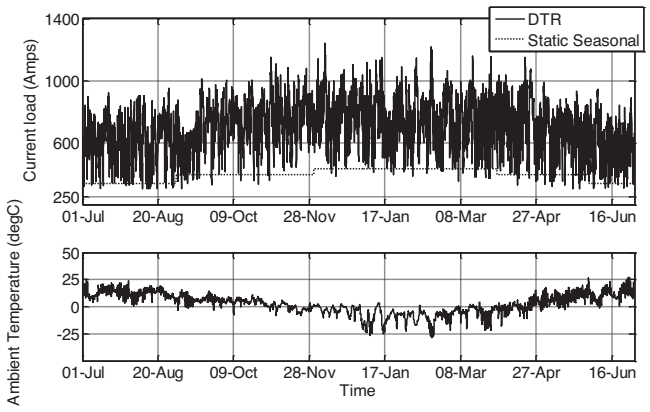

Fig. 5. RTTR vs Static rating for overhead bare line (July, 2008 to June, 2009).

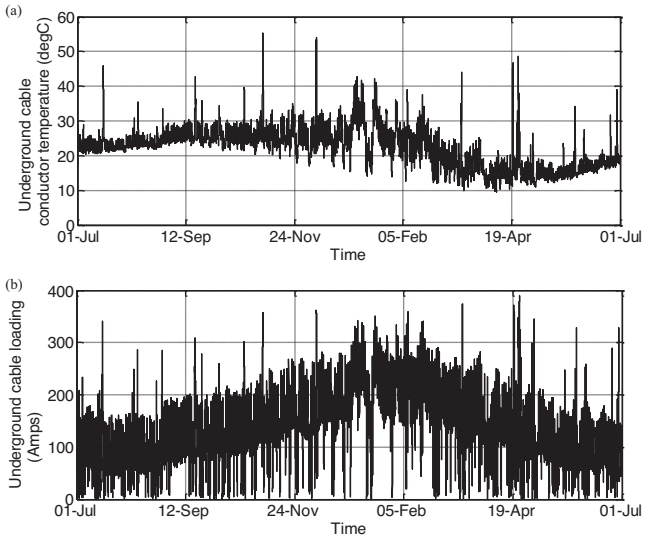

Fig. 6. One year conductor temperature (a) and the corresponding hourly loading profile (b) of an underground cable (July, 2008 to June, 2009).

conductor temperature of an underground cable installed inside unfilled conduit and loaded with current moderately influenced by the stochasticity of distributed generation. For underground cables, the model takes measured ground temperature as a reference. The ground temperature where the distribution system is operating varies slowly from +5.5 °C to +20.5 °C annually, following a sinusoidal shape. This variation is also reflected on the conductor temperature of the underground cable.

4. Load and generation modeling and forecasting

The forecasting of day ahead generation for photovoltaic panels as well as wind turbines requires weather variable forecasts. For the scope of this paper, the errors associated with wind, ambient temperature and solar irradiation forecasts are not included in the calculation. However, readily forecasted data is assumed to be attainable from metrological centers. Hence, the wind, ambient temperature and solar irradiation data used in this paper are considered to be ideal forecasts with zero errors. The time series model used for 24 h ahead load forecasting belongs to the auto regressive with exogenous inputs (ARX) model group. It incorporates the lagging effects of temperature as well as consumptions from the previous week, as formulated in (1). The load model and forecasting is performed for each secondary substation, with the assumption that it inherently includes the stochasticity of customer load profiles connected under each substation.

$$y_t = C + \sum_{i=1}^{3} \alpha_i Y_{i,t} + \sum_{j=1}^{4} \beta_j x_{j,t} + \sum_{k=1}^{2} \gamma_k D_{k,t} + \varepsilon_t \qquad (1)$$

$$\varepsilon_t \sim N(0, \sigma^2)$$

where y_t is the output (target variable); C is constant or the intercept of the model; $Y_{i,t}$: lagging output values.

They include:

- Previous Day Maximum Load
- Previous Week Same Hour Load, $Y_{i,t-168}$
- Previous Day Same Hour Load, $Y_{i,t-24}$

$D_{k,t}$ denotes external inputs (explanatory variables).
They include:

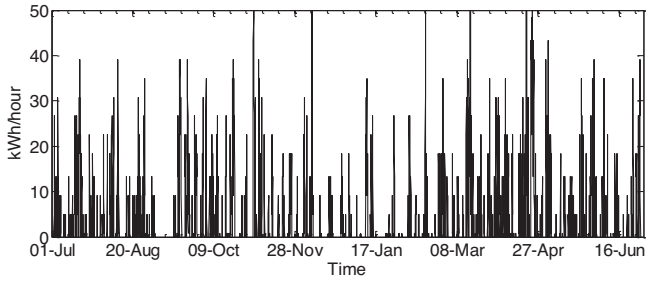

Fig. 7. One year hourly generated energy from a 50 kW wind turbine (kWh/h) (July, 2008 to June, 2009).

- same hour temperature
- amount of sun light (day length)
- Previous Hour Same Day Temperature
- Previous 2 Hour Same Day Temperature

$D_{k,t}$ denotes dummy variables
They include:

- weekday dummy variable
- weekend and holiday dummy variables

α_i, β_i and γ_k are coefficients estimated using ordinary least squares estimation. The lags are selected so that the error term ε_t is white noise.

4.1. Wind turbine model

A simple wind turbine model, which uses its nominal power, cut-in speed, speed of rated output and wind speed, is used to calculate the corresponding generated power. The model approximates the power characteristics curve of the wind turbine with two straight lines, and is given in Eq. (2). One year hourly weather data for wind speed was attained from the Finnish Meteorological Institute (FMI) [18]. For a 50 kW wind turbine the hour by hour generation profile for one year is plotted in Fig. 7.

$$P_{wind} = \begin{cases} S \cdot w_{meas} + K, & w_{cut\_in} < w_{meas} \text{ and } w_{nomin} > w_{meas} \\ P_{nomin}, & w_{meas} \geq w_{nomin} \end{cases} \qquad (2)$$

$$S = \frac{P_{nomin}}{w_{nomin} - w_{cut\_in}}$$

$$K = -S \cdot w_{cut\_in}$$

P_{nomin} is the rated power; w_{nomin} is the wind speed at rated power; w_{cut_in} is the cut-in wind speed (m/s); w_{meas} is the wind speed (m/s); S is the slope; K is the constant.

4.2. Solar panel model

A practical model developed by Jones and Underwood for the production of optimal output power from a photovoltaic module is used in this study [19]. The approach uses the simple relationships from the diode model of irradiance and temperature with short circuit current and open circuit voltage to calculate maximum power output. In Eq. (3), except for ambient temperature and solar irradiance values, all other values can easily be taken from the manufacturers' datasheet of the considered module. The one year hourly weather data for ambient temperature is from the Finnish Meteorological Institute (FMI), and the solar irradiation data is from the Solar Energy Services for Professionals (SoDa) website [18,20]. The

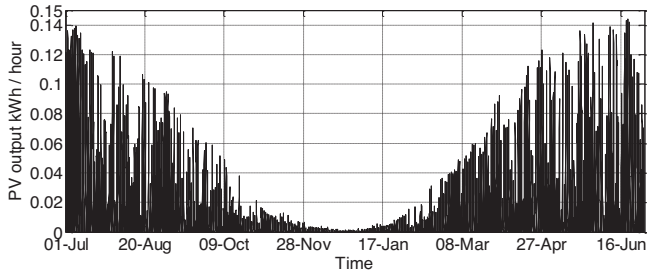

Fig. 8. One year hourly generated energy from a single 215 Wp solar panel (kWh/h) (July, 2008 to June, 2009).

hourly generation profile for a 215 Wp (peak) solar panel installed at 64.2° N, 27.7° E is plotted in Fig. 8.

$$P_{pv\_max} = FF \cdot \left(I_{sc} \cdot \frac{G}{G_{ref}}\right) \cdot \left(V_{oc} \cdot \frac{\ln(P_1 \cdot G)}{\ln(P_1 \cdot G_{ref})} \cdot \frac{T_{jref}}{T_j}\right)$$
$$FF = \frac{PV_{max}}{V_{oc} I_{sc}} \tag{3}$$
$$P_1 = \frac{I_{sc}}{G}$$
$$T_j = T_{air} + \frac{NOCT - 20}{80} \cdot S$$

T_j is the PV cell temperature (K); T_{jref} is the reference cell temperature (K); FF is the filling factor; S is the insolation (mW/cm^2); I_{sc} is the short circuit current (A); V_{oc} is the open circuit voltage (V); PV_{max} is the maximum power under Standard Test Condition (STC) (for our PV: irradiance of 1000 W/m^2 and cell temperature of 25 °C); T_{air} is the air temperature (degC); G is the irradiance (W/m^2); G_{ref} is the standard irradiance (W/m^2); PV_{max} is the maximum power under STC conditions (W); P_{pv_max} is the maximum power output (W).

5. Algorithm for RTTR and optimal power flow

The OPF is a technique deployed in power systems to address problems ranging from economic dispatch to loss minimization [21]. In this study the OPF function utilizes static rating or real-time thermal rating of the system to decide the permissible loads of network components. Whenever static rating or thermal violation is experienced, only curtailment of DGs or loads is considered as correction measures, as shown in the flow chart in Fig. 9. The objective for the OPF is to minimize the total cost of load and DG curtailment whenever ratings are exceeded. Within the scope of this paper, only the potential that a dynamic thermal rating function brings to a distribution network has been shown, especially with the increasing connection of distributed generation. Real-time network reconfiguration can also be an alternative remedy for network capacity violations, but it is not considered in the presented framework.

As shown in Fig. 9 there is a decision making step depending either on whether thermal violation or static rating violation is detected. The logic behind the limit violation decision is given in Table 3. Since the loading scenario in this study is hourly, the emergency limits of components with less than an hour loading limit are not an option. For oil immersed transformers, normal life expectancy occurs when a transformer is operating at 110 °C continuously. The normal life expectancy loading IEEE guide also allows up to 120 °C hotspot temperature and a corresponding 1.17 pu loading for a short period during the day. Besides, according to the IEEE guide, a planned loading beyond the nameplate rating is allowed up to 130 °C hotspot temperature or 1.27 pu loading [13]. In this analysis, however, the RTTR is chosen to operate within the normal life expectancy loading limit. Hence, a 110 °C limit is used during the comparison of 8 scenarios of DG penetrations (Table 4) and a 120 °C limit is used for identification of substation loading and DG penetration limits (Tables 6 and 7 respectively).

Table 3
Static loading thermal limits for decision making.

1 h maximum	OH (conductor)	UG (conductor)	TRAFO (hotspot)
Static rating	430 A	330 A	1600 kVA
Temperature	110 °C	90 °C	110 °C/120 °C

The algorithm shown in Fig. 9 is applied for 8 scenarios over a period of one year for different levels of DG (see Table 4). As the primary substation transformer rating is 40 MVA, it is used as the system capacity to decide the DG level. The solar panels are connected behind secondary substations whereas the wind turbines are connected to the MV network. The stressed network components are: secondary substation transformer at node 1, overhead line section 14 and underground cable section 12. The loadings and the respective thermal responses are analyzed for these components in the next section.

In the Finnish environment the solar panel yearly generation trend goes in the opposite direction to the actual consumption due to higher heating consumption in winter, which is also the darkest season. This trend is depicted in Fig. 10, showing the loading on transformer substation 12, where solar panels are connected to the LV side. The negative power implies solar panel generated power flowing to the MV network after fully supplying local loads. Since our load measurements are AMR based with 1 h resolution, the corresponding current loads on the line sections are also hourly, as shown in Fig. 11. Also shown in Fig. 11, the thermal violations in this study were assessed by the real-time state of hotspot temperatures not from steady state temperature.

5.1. Optimal power flow

The optimization routine is called whenever any violation in static or real-time thermal rating limits occurs. The choices considered to counter rating violations in this study are load curtailment and DG curtailments. An hourly NordPool market price is used as the cost of DG curtailment and an average cost is used for load curtailment, as presented in [22]. Hence the OPF tries to minimize the total cost of load and generation curtailments while keeping loadings under the limits of the specific hour. Real-time network reconfiguration is not realized in today's distribution networks, however, it will be an interesting research topic in relation to stochastic loading and real-time thermal ratings. On the other hand, network investment could also be considered as an alternative solution; nevertheless, provided that DG and load curtailment costs are quantified it will be a straightforward comparison to make. The formulation of the OPF is provided in (4).

$$Minimize \sum_i (\rho_{lc}^{i,t} P_{lc}^{i,t} + \rho_{gc}^{i,t} P_{lvgc}^{i,t} + \rho_{gc}^{i,t} P_{mvgc}^{i,t}) \tag{4}$$

where t and i are indices for time span and buses. $\rho_{lc}^{i,t}$ is compensation cost for curtailed load $P_{lc}^{i,t}$ and $\rho_{gc}^{i,t}$ is compensation cost for curtailed low voltage side generation ($P_{lvgc}^{i,t}$) and medium voltage side generation ($P_{mvgc}^{i,t}$) at time span t and bus i. The objective function (4) is subjected to the following constraints:

$$P_f^{ij,t} = -Y_f^{ij} V_i^t V_j^t \cos(\delta_i^t - \delta_j^t + \theta_f^{ij}) + Y_f^{ij} V_i^{t^2} \cos(\theta_f^{ij}) \tag{5}$$

$$Q_f^{ij,t} = -Y_f^{ij} V_i^t V_j^t \sin(\delta_i^t - \delta_j^t + \theta_f^{ij}) + Y_f^{ij} V_i^{t^2} \sin(\theta_f^{ij}) \tag{6}$$

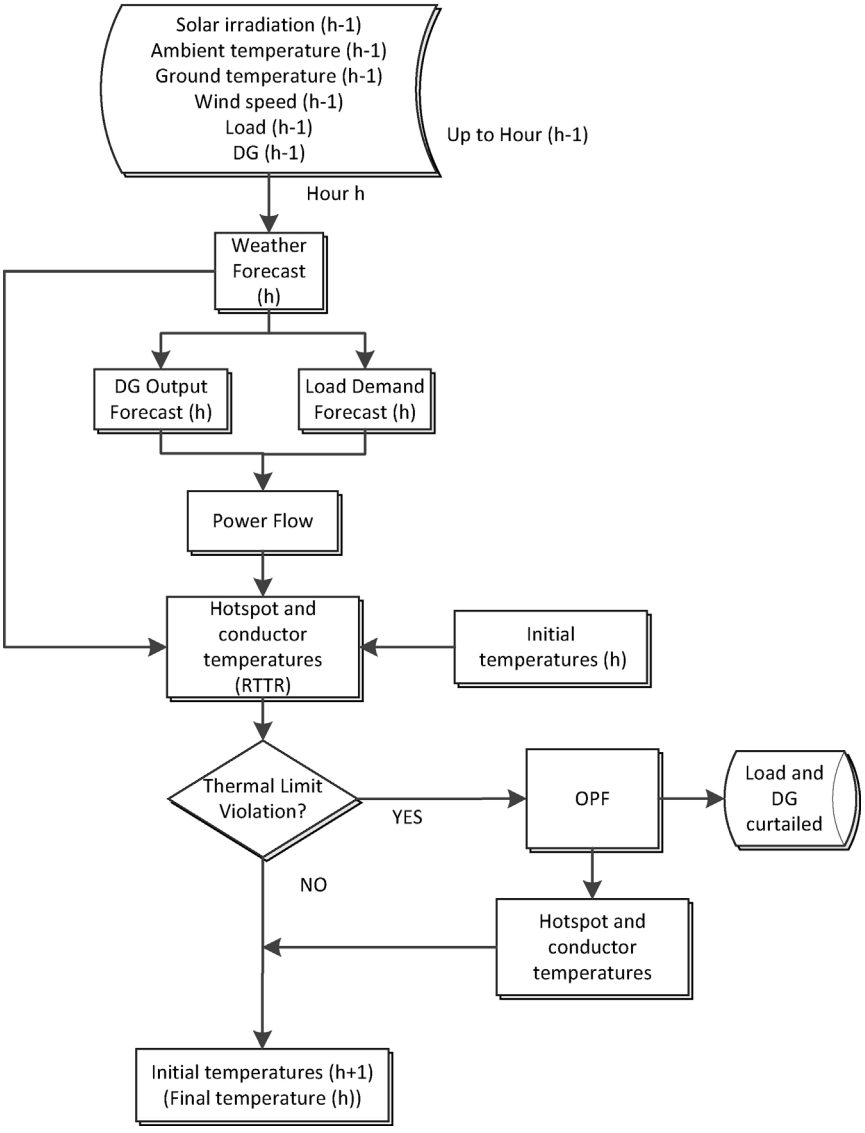

Fig. 9. Real-time thermal rating framework for hour ahead dispatching.

Table 4
DGs prevalence scenarios for MV distribution network operating radially.

	DG level (out of 40 MVA)	DG cumulative maximum (MVA)	WIND			SOLAR		
			Node 12 (number of 50 kW turbines)	Node 14 (number of 50 kW turbines)	Total (kVA)	Node 10 (number of 215 Wp solar panels)	Node 12 (number of 215 Wp solar panels)	Total (kVA)
Scenario#1	0	0	0	0	0	0	0	0
Scenario#2	50%	20	107	285	19,600	1017	1763	400
Scenario#3	100%	40	214	570	39,200	2034	3525	800
Scenario#4	110%	44	235	627	43,120	2237	3878	880
Scenario#5	120%	48	257	684	47,040	2441	4231	960
Scenario#6	150%	60	321	855	58,800	3051	5288	1200
Scenario#7	200%	80	428	1140	78,400	4068	7051	1600
Scenario#8	315%	126	675	1799	123,676	6418	11,125	2524

$$S_f^{ij,t} = \sqrt{P_f^{ij,t^2} + Q_f^{ij,t^2}} \tag{7}$$

$$P_s^{i,t} = P_l^{i,t} - P_{lc}^{i,t} - P_{lvg}^{i,t} + P_{lvgc}^{i,t} \tag{8}$$

$$Q_s^{i,t} = Q_l^{i,t} - Q_{lc}^{i,t} - Q_{lvg}^{i,t} + Q_{lvgc}^{i,t} \tag{9}$$

$$S_s^{i,t} = \sqrt{P_s^{i,t^2} + Q_s^{i,t^2}} \tag{10}$$

$$P_{mvg}^{i,t} - P_{mvgc}^{i,t} - P_s^{i,t} - \sum_j P_f^{ij,t} = 0 \tag{11}$$

$$Q_{mvg}^{i,t} - Q_{mvgc}^{i,t} - Q_s^{i,t} - \sum_j Q_f^{ij,t} = 0 \tag{12}$$

$$\underline{V_i} \le V_i^t \le \overline{V_i} \tag{13}$$

Table 5
Comparison of real-time thermal rating and static rating for different penetration levels of DGs.

DG scenario	Number of hours in year		Undelivered energy STATIC rating (MWh)		Undelivered energy RTTR (MWh)	
	Violations of static rating	Violations of RTTR	Load curtailed	DG curtailed	Load curtailed	DG curtailed
S1	0	0	0	0	0	0
S2	54	0	0	77.65	0	0
S3	430	191	0	2243.73	0	969.97
S4	433	258	0	2993.36	0	1434.80
S5	603	294	0	3858.65	0	1972.13
S6	618	440	0	6881.58	0	4046.98
S7	893	624	0	13,111.73	0	8822.90
S8	1295	1087	0	31,224.89	0	23,594.88

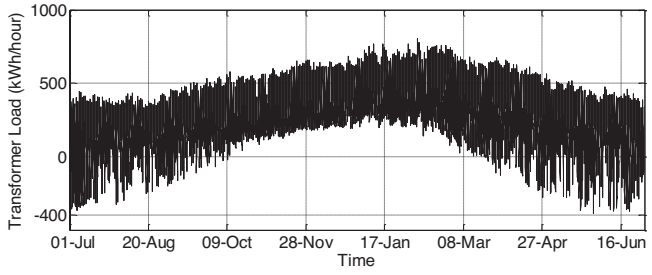

Fig. 10. Secondary substation 12 transformer load for scenario#6 (July, 2008 to June, 2009) (negative power is associated with LV connected solar panels power supply to MV network).

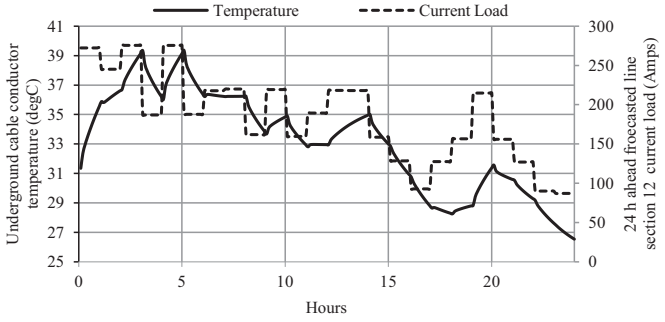

Fig. 11. Line section 12 underground cable forecasted load and the corresponding conductor temperature for scenario#3.

$$0 \le P_{lc}^{i,t} \le P_{l}^{i,t} \tag{14}$$

$$0 \le P_{lvgc}^{i,t} \le P_{lvg}^{i,t} \tag{15}$$

$$0 \le P_{mvgc}^{i,t} \le P_{mvg}^{i,t} \tag{16}$$

$$P_{lc}^{i,t} Q_{l}^{i,t} - Q_{lc}^{i,t} P_{l}^{i,t} = 0 \tag{17}$$

$$P_{lvgc}^{i,t} Q_{lvg}^{i,t} - Q_{lvgc}^{i,t} P_{lvg}^{i,t} = 0 \tag{18}$$

$$P_{mvgc}^{i,t} Q_{mvg}^{i,t} - Q_{mvgc}^{i,t} P_{mvg}^{i,t} = 0 \tag{19}$$

where f and j are indices for feeders and buses. $P_{l}^{i,t}(Q_{l}^{i,t})$, $P_{g}^{i,t}(Q_{g}^{i,t})$, and $P_{s}^{i,t}(Q_{s}^{i,t})$ are load, generation, and injected active (reactive) powers at time t and bus i. $P_{lvg}^{i,t}(Q_{lvg}^{i,t})$ and $P_{lvgc}^{i,t}(Q_{lvgc}^{i,t})$ are LV side generation and curtailment of active(reactive) power. $P_{mvg}^{i,t}(Q_{mvg}^{i,t})$ and $P_{mvgc}^{i,t}(Q_{mvgc}^{i,t})$ are MV side generation and curtailment of active(reactive) power. δ_{i}^{t} is the voltage angle and θ_{f}^{ij} is the power flow angle. V_{i}^{t} is the voltage magnitude at bus i and time t, respectively, whose limits are specified in (13), and $S_{f}^{ij,t}$ in (7) is the apparent power of feeder f between buses i and j at time t. $P_{s}^{i,t}$, $Q_{s}^{i,t}$ and $S_{s}^{i,t}$ are the active, reactive and apparent powers injected at bus. Finally, $P_{f}^{ij,t}(Q_{f}^{ij,t})$ is the active (reactive) power flowing at time t through feeder f connecting bus i to bus j. (5) and (6) calculate the active and reactive power flowing through the feeders. (7) calculates the apparent power flowing through the feeders. (8) and (9) calculates the active and reactive power absorbed from the buses. (10) calculates the apparent power absorbed from buses. (11) and (12) are the active and reactive power balance at the buses. (13) forces the voltage magnitudes at the buses to be within an acceptable range. (14) ensures that load curtailment at each bus is less than the total load at that bus. (15) and (16) ensure that the generation curtailment at each bus (low voltage and medium voltage) is less than the total generation at that bus (low voltage and medium voltage). (17)–(19) guarantee

Table 6
Percentage of load increment upto the static and RTTR rating limits for the 16 secondary substations.

Substation number	Annual peak demand (pu)	% of additional load increment limits		
		Static rating (1.17 pu)	RTTR (120°)	Difference
SUB#1	1.2	Overloaded	10.00%	10.00%
SUB#2	0.970	20.64%	40.00%	19.36%
SUB#3	0.635	84.33%	100.00%	15.67%
SUB#4	0.839	39.50%	60.00%	20.50%
SUB#5	0.317	269.46%	310.00%	40.54%
SUB#6	0.760	53.89%	70.00%	16.11%
SUB#7	0.810	44.42%	60.00%	15.58%
SUB#8	0.578	102.41%	170.00%	67.59%
SUB#9	0.533	119.69%	150.00%	30.31%
SUB#10	0.415	181.84%	230.00%	48.16%
SUB#11	0.322	262.86%	530.00%	267.14%
SUB#12	0.503	132.75%	170.00%	37.25%
SUB#13	0.283	312.70%	400.00%	87.30%
SUB#14	0.382	206.57%	260.00%	53.43%
SUB#15	0.480	143.93%	170.00%	26.07%
SUB#16	0.371	215.53%	240.00%	24.47%

that the power factor remains the same after and before either load or generation curtailment.

Although the formulation presented in (4) is general, a DC power flow is used in both pre-optimization load flow and the optimal power flow of the test case scenarios (see Fig. 9). DC power flow is used for its computational simplicity. It should be noted that the accuracy of the DC power flow model is not of concern, since the focus of this paper is on capacity limit violations (not under voltage). Besides, for the test network utilized in this study, the difference between AC and DC power flow has been checked to be trivial. The real-time thermal rating is solved in MATLAB whereas the optimal power flow is solved by General Algebraic Modeling System (GAMS).

6. Comparison between distribution system static rating and real-time thermal rating

For the static rating a constant current limit is set, where the steady state temperature of the conductor, in the case of overhead lines and cables, and the hotspot temperature in the case of transformers are set to their maximum according to manufacturers' datasheets. However, in RTTR, the conductor and hotspot temperature are monitored based on thermal models to decide loading limits. Therefore, in static rating constant loading limits (at least seasonal limits) are used whereas in RTTR time varying loading limits are set. Hence, the overall loading capacity increment, for example, of overhead lines is tightly linked to the ambient temperature, wind speed and solar irradiation. In Finnish weather conditions for a 20 kV bare overhead line, about 58% more delivered energy in one year would be possible in the case of real-time thermal rating rather than static rating. For underground cables, however, the time constant is too long to react to instantaneous loading and DG output profile. Hence temporary overloading, especially in the case of contingencies, is viable as long as it is followed by an extended period of low loading. Transformers lie somewhere in between, where whether it is installed inside a room or in the outside environment influences the real-time thermal rating. In this study, an indoor installation is considered since our test network is for a sub-urban area. Hence, the real-time thermal rating for transformers focuses more on overseeing upcoming thermal violations than setting the maximum hourly load limit for the next 24 h.

Usually, it is not probable that the best DG installation area will be near highly populated loads, especially in the case of wind turbines. In the test network the most problematic line section is the overhead line section 14. It supplies the wind turbine generations connected to the MV side. In the case of RTTR implementation, there is no major overloading up to a 120% penetration level of DGs in the network. However, for static rating the expected energy not served is remarkably high at only a 100% penetration level. Underground cable line section 16 shows 2.5 times more unserved energy in the case of static rating rather than RTTR. Although for most line sections in the distribution network loading has decreased with increasing penetration level of DGs, those components near to DG installations experience highly volatile loading and even increased temporary overloading. Assuming more DGs are to be installed in the already selected favorable area, RTTR can defer network investment by allowing 10–20% more DG penetration than the static rating can handle. This can be realized by installing RTTR capability which increases DG installation potential before the need for additional network investment. Also for the installed DG, the efficient utilization of the generated renewable energy increases by the same percent. This can be achieved with negligible loss of life (see Table 5 and Fig. 12). Nevertheless, there is also mechanical stress imposed by highly stochastic loading on network components. This issue needs to be investigated, especially for termination

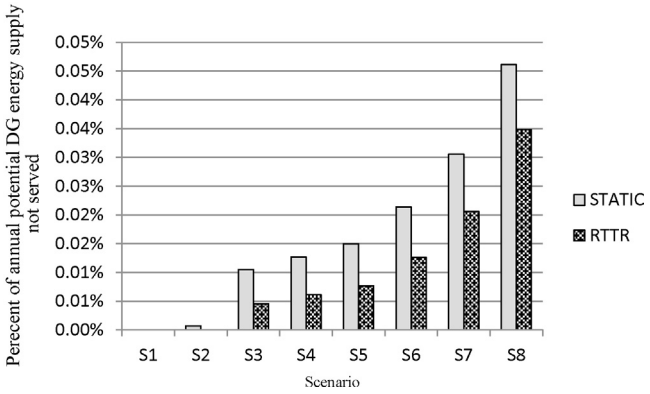

Fig. 12. Unserved DG generation due to capacity limit with RTTR and Static rating.

points and joints in high and medium voltage underground line sections connecting wind turbines [23]. In Table 5, the cumulative DG unserved energy in the distribution network is presented. The unserved energy is calculated by solving the OPF model which was described and formulated earlier.

The differences between the secondary substations in Tables 6 and 7 are due to the types of households connected affecting the load factor and shape very distinctly based on their proportions in Table 2. Without installation of DGs, the loads are increased starting from the existing annual peak load up to the static rating and RTTR limits. According to the results in Table 6, on average RTTR has a 48% greater loading possibility of the existing load compared to the static rating limits. In an additional analysis, keeping the existing load constant, the penetration of DGs (solar panels) under each secondary substation was increased up to the secondary substation transformer static rating and RTTR limit as shown in Table 7. In general there is higher potential for connecting more DGs than the potential of load increment, as can be seen in Tables 6 and 7. When we look into hourly annual peak distributed generation and load demand, even if they have the same per-unit values, the historical and future generation or load have very distinct profiles. The stochasticity in distributed generation helps the RTTR since the occasional spikes in generation usually occur for only a very short period compared to the time constants of the components, as shown in Table 7. RTTR allows a margin of approximately 40% more capacity compared to static ratings, for both additional loading and DG integrations, as the results in Table 7 show.

The objective function in (4) calculates the total cost of load curtailment using average cost and the cost of DG curtailment based on the Nordpool hourly spot price. Comparing the total yearly costs for the RTTR and static rating systems, the saved cost is plotted in Fig. 13. The monetary benefit of RTTR increases exponentially with the penetration level of DGs, as shown in Fig. 13. The extra network capacity released by the RTTR system has also some indirect impacts on aspects of distribution networks' operation such as dispatch of resources and network reconfiguration, as well as planning aspects such as postponing investments. Hence, the overall economic analysis is a valuable future research topic in its own right.

With regard to the practical deployment of the RTTR system, measurement sensor installation and existing EMS system compatibility are needed. In [5], it is mentioned that EPRI's dynamic thermal circuit rating program will run on a PC that is networked to the SCADA/EMS system where the required measurements are accessed. A field trial thermal controller installed on a Scottish distribution network deployed relays to collect weather data such as wind speed and direction, ambient temperature, soil temperature, soil moisture and solar irradiation [11]. For the RTTR system to be

Table 7
Percentage of DG installment capacity from annual peak up to the static and RTTR rating limits for the 16 secondary substations.

Substation number	Percentage of Solar panel installment compared to the peak load connected to each secondary substation			
	Annual peak demand (pu)	Static rating (1.17 pu)	RTTR (120°)	Difference
SUB#1	1.2	90.00%	170.00%	80.00%
SUB#2	0.970	130.00%	150.00%	20.00%
SUB#3	0.635	200.00%	230.00%	30.00%
SUB#4	0.839	150.00%	170.00%	20.00%
SUB#5	0.317	390.00%	440.00%	50.00%
SUB#6	0.760	170.00%	240.00%	70.00%
SUB#7	0.810	160.00%	180.00%	20.00%
SUB#8	0.578	220.00%	300.00%	80.00%
SUB#9	0.533	240.00%	270.00%	30.00%
SUB#10	0.415	300.00%	340.00%	40.00%
SUB#11	0.322	370.00%	420.00%	50.00%
SUB#12	0.503	250.00%	280.00%	30.00%
SUB#13	0.283	430.00%	490.00%	60.00%
SUB#14	0.382	320.00%	370.00%	50.00%
SUB#15	0.480	260.00%	340.00%	80.00%
SUB#16	0.371	330.00%	380.00%	50.00%

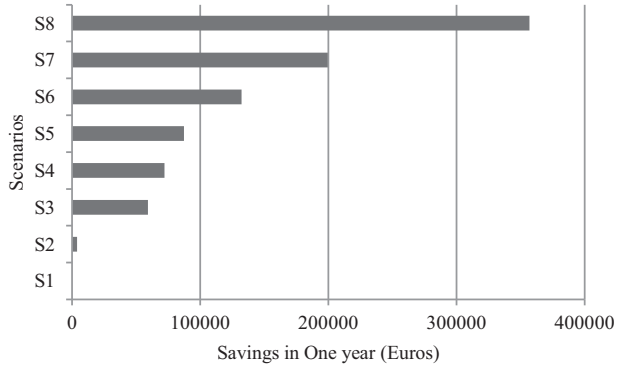

Fig. 13. One year cumulative cost savings of curtailed load and DG generation for real-time DTR system compared to static rating system.

used for real-time network reconfiguration or DG control, a high resolution of such weather data has to be communicated with the RTTR system hosting computer. Also, to implement and harness the benefits of the above control strategies based on real-time thermal rating for smart distribution networks, reliable communication infrastructures are needed, as is pointed out in [24]. Based on the quality of the available measurements there might be a need for thermal state estimation programs to be integrated with distribution network distributed state estimation algorithms.

7. Conclusion

This study quantifies the benefits of real-time thermal rating in accommodating new DGs and utilizing installed ones. The benefits of an RTTR system are quantified with the simulation of a typical active distribution network supplying variety of household types and with different scenarios of DG penetration level. The introduction of real-time thermal rating in an active distribution network management system enhanced the loading capacity significantly compared to static rating. This has been revealed through an increased utilization of installed DGs and through better integration potential for new DGs. The increment of distribution network loading capacity with RTTR can be achieved without the compromise of aging the network components. In this study, it was assumed that voltage drop is not a limiting factor in the considered network. This assumption may not hold in the case of very heterogeneous loads and DGs connected to only some of the substations with longer feeders. The issue of voltage management in such cases is a subject for further study. The study also emphasized the need for a deeper investigation of the stochasticity of loading due to intermittent DG output and its impact on the mechanical strength of components.

The implementation of price and network based demand response programs, the pervasiveness of electric vehicles, the increasing installation of DGs, the rising customer load base of urban areas and other emerging factors are creating a distribution network loading curve which is stochastic in nature and previously unseen in shape. Hence, static distribution network rating is no longer a good enough network management tool. Rather, utilities need to adapt to the dynamism of load and generation behavior by applying programs such as RTTR for efficient and secure network operation.

Acknowledgements

The authors of this paper would like to acknowledge that this work is jointly funded by the Aalto Energy Efficiency Research Program (AEF) through the SAGA and STEEM projects and, the SGEM project.

Appendix A.

Line and cable parameters

	Res (Ω/m)	React (Ω/m)	Rated current (A)
Underground cable (240Wiski)	0.000138	0.00011	330
Overhead line (Al132)	0.000279	0.000344	430

References

[1] R.C. Dugan, T.E. McDermott, Operating conflicts for distributed generation on distribution systems, in: IEEE Rural Electric Power Conference, 2001, A3–1.
[2] S.C.E. Jupe, P.C. Taylor, Distributed generation output control for network power flow management, IET Renew. Power Gener. 3 (2008) 371–386.
[3] R.F. Arritt, R.C. Dugan, Distribution system analysis and the future smart grid, IEEE Trans. Ind. Appl. 47 (2011) 2343–2350.
[4] A. Neumann, P. Brinckerhoff, Unlock distribution capacity using dynamic thermal ratings, Energize (2008) 18–19.
[5] D.A. Douglass, D.C. Lawry, A.A. Edris, E.C. Bascom, Dynamic thermal ratings realize circuit load limits, IEEE Comput. Appl. Power 13 (2000) 38–44.
[6] A. Michiorri, P.C. Taylor, Forecasting real-time rating for electricity distribution networks using weather forecast data, in: 20th International Conference on Electricity Distribution, CIRED, 2009, pp. 1–4.
[7] R.C. Dugan, T.E. McDermott, G.J. Ball, Planning for distributed generation, IEEE Ind. Appl. Mag. 2 (2001) 80–88.
[8] R.A. Walling, R. Saint, R.C. Dugan, J. Burke, L.A. Kojovic, IEEE summary of distributed resources impact on power delivery systems, IEEE Trans. Power Deliv. 23 (2008) 1636–1644.
[9] R.A.F. Currie, G.W. Ault, J.R. McDonald, Methodology for determination of economic connection capacity for renewable generator connections to distribution

networks optimized by active power flow management, IEE Proc. Gener. Transm. Distrib. 153 (2006) 456–462.
[10] A. Borghetti, M. Bosetti, S. Grillo, S. Massucco, C.A. Nucci, M. Paolone, F. Silvestro, Short-term scheduling and control of active distribution systems with high penetration of renewable resources, IEEE Syst. J. 4 (2010) 313–322.
[11] H.T. Yip, C. An, G.J. Lloyd, P. Taylor, Dynamic thermal rating and active control for improved distribution network utilization, Dev. Power Syst. Prot. (2010) 1–5.
[12] R.J. Millar, E. Saarijärvi, M. Lehtonen, M. Hyvärinen, J. Niskanen, P. Hämäläinen, Electricity distribution network planning algorithm based on efficient initial and radial-to-full network conversion, Int. Rev. Electr. Eng. 8 (2013) 1076–1090.
[13] IEEE Guide for Loading Mineral-Oil-Immersed Transformers, IEEE Std C57. 91-2011.
[14] M.Z. Degefa, M. Lehtonen, R.J. Millar, Comparison of air-gap thermal models for MV power cables inside unfilled conduit, IEEE Trans. Power Deliv. 27 (2012) 1662–1669.
[15] M.Z. Degefa, R.J. Millar, M. Lehtonen, P. Hyvönen, Dynamic thermal modeling of MV/LV prefabricated substations, IEEE Trans. Power Deliv. 29 (2014) 786–793.
[16] IEEE Standard for Calculating the Current – Temperature Relationship of Bare Overhead Conductors, IEEE Std. 738-2006.
[17] R.J. Millar, M. Lehtonen, A robust framework for cable rating and temperature monitoring, IEEE Trans. Power Deliv. 21 (2006) 313–321.
[18] FMI – Finnish Meteorological Institute: http://en.ilmatieteenlaitos.fi/
[19] A.D. Jones, C.P. Underwood, A modeling method for building-integrated photovoltaic power supply, Build. Serv. Eng. Res. Technol. 23 (2002) 167–177.
[20] Solar Energy Services for Professionals, http://www.soda-is.com/eng/index.html
[21] M.Z. Degefa, R.J. Millar, M. Koivisto, M. Humayun, M. Lehtonen, Load flow analysis framework for active distribution networks based on smart meter reading system, Engineering 5 (2013) 1–8.
[22] S. Kazemi, Reliability Evaluation of Smart Distribution Grids (Ph.D. Dissertation), Depts. Elec. Eng., Sharif University of Technology and Aalto University, 2011 http://lib.tkk.fi/Diss/2011/isbn9789526042411/
[23] J.Z. Hansen, Failure in MV joints (XLPE cable) in heavy loaded cable systems connecting large windmills to the distribution system, in: NORDAC, Danish Energy Association, 2012.
[24] G. Celli, E. Ghiani, F. Pilo, G.G. Soma, Reliability assessment in smart distribution networks, Electr. Power Syst. Res. 104 (2013) 164–175.